Steam exploded wheat straw fibers as reiforcing for polypropylene based composites. Characterization and properties.

Maurizio Avella, Claudio Bozzi, Ramiro Dell'Erba, Bonaventura Focher, Annamaria Marzetti, Ezio Martuscelli

Italian National Agency for New Technologies, Energy and Sustainable Economic Development

http://www.enea.it/en
http://robotica.casaccia.enea.it/index.php?lang=en

This paper is a pre-print. The final paper is available on:

Die Angewandte Makromoleculare Chemie „Steam exploded wheat straw fibers as reiforcing for polypropilene based composites. Characterization and properties.“ M. Avella, C. Bozzi, R.dell’Erba, B. Focher,A. Marzetti and E. Martuscelli V. 233, pag.149-166

[1] Istituto di Ricerca e Tecnologia delle Materie Plastiche C. N. R.,
Via Toiano 6, 80072 Arco Felice (Napoli), Italy
[2]Consorzio sulle Applicazioni dei Materiali Plastici e per i problemi di Difesa dalla Corrosione, via P. Castellino 111, 80100 Napoli, Italy
[3] Stazione Sperimentale per la Cellulosa, Carta e Fibre Tessili Vegetali ed Artificiali, Piazza Leonardo da Vinci, 26-20133 Milano, Italy

Steam-exploded wheat straw fibers as reinforcing material for polypropylene-based composites

Characterization and properties

Maurizio Avella[1], Claudio Bozzi[3], Ramiro dell'Erba[2], Bonaventura Focher[3], Annamaria Marzetti[3], Ezio Martuscelli[1]*

SUMMARY:

Composites of wheat straw fibers with polypropylene (iPP) and maleic anhydride modified polypropylene (iPPMA) were prepared.

Before being mixed with polypropylene matrices, the wheat straw fibers were subjected to a steam explosion process that induces morphological and structural changes in lignocellulosic materials. Such changes are able to enhance the interactions with the thermoplastic matrix.

Compared with iPP, the modified matrix (iPPMA) has shown higher mechanical performances (tensile and impact behavior) and a remarkable decrease of water absorption, that is one of the main drawbacks of natural fiber composites.

Finally, the presence of covalent bonds between maleic anhydride and steam-exploded (STEX) fibers, by means of an esterification reaction, produced during the melt-mixing process, can explain the resulting good interfacial adhesion found in iPPMA-based composites.

ZUSAMMENFASSUNG:

Aus Weizenstrohfasern und Polypropylen (iPP) bzw. mit Maleinsäureanhydrid modifiziertem Polypropylen (iPPMA) wurden Composite hergestellt. Die Weizenstrohfasern wurden vor dem Einmischen in die Polypropylenmatrix einem Dampfexplosionsprozeß unterworfen, der bei Lignocellulosematerialien morphologische und strukturelle Veränderungen bewirkt, die zu einer Verbesserung der Wechselwirkungen mit der thermoplastischen Matrix führen können. Die modifizierte iPPMA-Matrix weist im

* Correspondence author.

ten) und eine bemerkenswerte Verringerung der Wasseraufnahme, einer der Hauptnachteile von Compositen mit Naturfasern, auf. Die gute Grenzflächenhaftung in den iPPMA-Compositen kann mit den beim Mischen der Fasern mit der Polymerschmelze gebildeten kovalenten Esterbindungen zwischen den Maleinsäureanhydrid-Segmenten und den dampfbehandelten Fasern erklärt werden.

1 Introduction

In the last years, natural fibers have emerged as renewable and cheap reinforcement to make structural composite materials[1].

Lignocellulosics-based natural fibers posses high specific properties, good mechanical properties and are abundantly available. Among the natural materials, wheat straw fibers are in surplus inside the European Community and thus they can be used as a very cheap filler for composites[2].

A strong performance of these fibers as reinforcement for synthetic materials is dependent on their cellulose content and on realized fiber/matrix interfacial adhesion[3–5].

In previous works it was shown that fractions of lignocellulosic materials, rich in cellulose content and having also high reactivity, can be obtained by the steam explosion process (S.E.P.)[6]. This treatment allows to break the wood cell wall and makes possible a fractionation of lignocellulosic material into its main components: cellulose, lignin and hemicelluloses; furthermore, by eliminating the latter two, stronger fibers containing a high percentage of cellulose (60–70%) can be produced. Moreover, the modifications induced by steam explosion on the morphology of straw permit to increase the surface area of the cellulose component, giving rise to a highly reactive material[7–10].

In the present paper, STEX straw fibers derived from wheat were used to prepare composites having as matrix two commercial polypropylenes: an isotactic polypropylene sample (iPP) and a modified isotactic polypropylene sample, obtained by grafting on the backbone a small amount of maleic anhydride (iPPMA)[11].

The thermal, mechanical and morphological behavior of the two series of composites was investigated and compared; moreover the resulting interfacial adhesion was examined by scanning electron microscopy (SEM) and infrared Fourier Transform spectroscopy.

Finally, the resistance to water of the composites was also tested by swelling measurements to assess the strength of the interphase between the polypropylene (iPP and iPPMA) and the exploded straw fibers.

2.1 Materials

The polypropylene (iPP) and the maleate-modified polypropylene (iPPMA) (Himont) were used as received, and some characteristics are shown in Tab. 1.

The wheat straw fibers were subjected to steam explosion treatment[6] in a laboratory apparatus (Delta lab EC 300) by using explosion conditions reported elsewhere[7].

Before use the fibers were stored in a stove at a temperature of 55 °C under high vacuum for enough time to permit the release of the water adsorbed during the steam explosion process. The characteristics of the materials are reported in Tab. 1.

Tab. 1. Characteristics of polypropylenes used.

Materials	Density ($g \cdot cm^{-3}$)	η [a] ($dL \cdot g^{-1}$)	Maleic anhydride content (wt.-%)	
			grafted	free
iPP	0.9	0.97	0	0
iPPMA	0.9	1.09	1.6	0.65

[a] 1,2,4-Trichlorbenzene, 135 °C.

2.2 Specimens preparation

The fibers were chopped into short-length filaments (max ≅ 1 mm) using an electric grinding mill. Afterwards they were mixed with polypropylene using a Brabender-like apparatus (Rheocord EC, Haake Inc.) operating at 190 °C for 10 min.

The prepared composites contain 0, 10, 20, 30 or 50 wt.-% fibers (the volume fraction was consequently varied from 0 to 25.64%).

Afterwards the material was chopped in the electric grinding mill and dried in a stove 24 h at 55 °C.

The milled material was placed between two Teflon sheets in a 1.0 mm (or 3.5 mm for fracture tests) thick steel frame. The whole system was inserted between the plates of a hydraulic press heated at 190 °C and kept without any applied pressure for 7 min, allowing complete melting. After this period a pressure of 10 MPa was applied for 3 min. The sample was cooled following the curve shown in Fig. 1.

Previous thermogravimetric analysis had established that under such processing conditions no appreciable thermomechanical degradative effects were detected.

Two different classes of sheets of different thickness were prepared: 3.5 mm for fracture tests and 1.0 mm for tensile tests.

Eight types of samples have been prepared and named with the following code: iPP, iPP80/20, iPP50/50 (for neat iPP), iPPMA, iPPMA90/10, iPPMA80/20, iPPMA70/

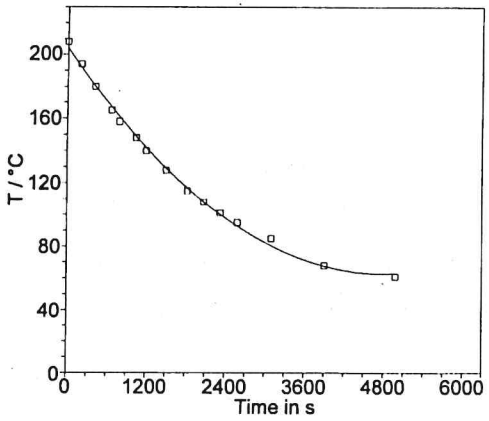

Fig. 1. Experimental curve of cooling rate used to prepare the samples by compression molding.

30, iPPMA50/50 (for maleate-modified iPP). The second number stands for the perceptually weight content of STEX straw fibers.

To perform tensile and fracture tests the sheets successively were cut by a mill.

Prior to fracture testing, the samples were notched as follows: first a blunt notch was produced by using a machine with a V-shaped tool, and then a sharply notch of 0.2 mm depth was made by a razor blade fixed to a micrometric apparatus. The final value of notch depth was measured after fracture by using an optical microscope.

An attempt to blend iPPMA with untreated straw (not steam-exploded) was also effected for iPPMA80/20, but the resulting material was lacking in compactness showing that no cohesive forces between the two components were present.

2.3 Techniques

The apparent melting temperatures (T_m) and the crystallinity indices (X_c) for all the iPP samples prepared were determined by means of a differential scanning calorimeter (DSC) Mettler TA-3000 equipped with control and programming unit (microprocessor TC-10), operating under nitrogen atmosphere and working with a precision of $\pm 0.2\,^{\circ}C$ and 5% on the X_c values, respectively.

The melting temperature observed (T_m) and the apparent enthalpy (ΔH^*) of each sample were obtained from the maxima and the area of the melting peaks, respectively. The crystallinity indices of the samples were calculated by the following relation:

$$X_c = \Delta H^* / \Delta H^\circ$$

where ΔH° is the specific heat of fusion of 100% crystalline iPP, taken as 209 J g^{-1} [12].

All the measurements on the samples of about 8–10 mg weight were performed by using a scan rate of 20 °C/min.

The mechanical behavior of samples obtained by compression molding was examined by tensile tests which were performed according to the ASTM D638 standard (samples of type IV) by using an Instron machine (model 1122) at a crosshead speed of 10 mm min^{-1}.

Fracture tests were carried out on a Charpy Instrument Pendulum (Ceast Autographic Pendulum MK2) at an impact speed of 1 m s^{-1} (ASTM D256). Samples with a notch depth-to-width ratio of 0.3 and a span test of 48 mm (6.0 mm wide and 60 mm long) were fractured at room temperature. The relative curves of energy and load plotted versus time were recorded, and the critical strain energy release, G_c, and the critical stress intensity factor, K_c, were calculated according to the Linear Elastic Fracture Mechanics (LEFM) theory[13, 14].

The fiber matrix adhesion and morphological investigations were carried out by using a Philips 501 SEM on fracture surfaces obtained by tensile and fracture tests; the samples for SEM observation were metallized by means of a Polaron sputtering apparatus with Au-Pd alloy.

The infrared spectra were obtained on a Bruker IFS 66 FT-IR spectrometer, using KBr pellets. The reproducibility of the spectra was verified on two preparations of ground samples. The ground mixture was dried at 70 °C under vacuum for 16 h before pressing. Between 16 and 100 scans were taken with a resolution of 4 cm^{-1}.

In order to visualize details in the bands shape and the unresolved band components, the Fourier selfdeconvolution (FDS) procedure was applied using Bruker software with the methods of Kauppinen et al.[15]. To avoid side lobes and preserve the constancy of the sample band areas, the value chosen for the half-width Lorentzian line and resolution enhancement factor were 13–15 and 1.3 cm^{-1}, respectively.

The signal-to-noise ratio was better than 500 and the best quantitative information was obtained from the fitting of the deconvoluted spectra using "Fit", a Fortran program in Bruker software using an interactive procedure.

Dynamic-mechanical measurements were carried out by means of a dynamic thermal analyzer (DMTA MK III Polymer Labs.) operating in single cantilever bending mode (strain $< 0.1\%$) at a frequency of 1 Hz. The samples in the form of small bars (15 × 5 × 1) mm were investigated in the temperature range from $-80\,^{\circ}C$ to $120\,^{\circ}C$ with a heating rate of 2 °C/min.

The resistance of the composites reinforced with STEX straw against wet conditions was examined by immersion in water of the tensile specimens for one month. Subsequent measurements of the amount of water absorbed (increase in weight) and the relative residual tensile properties were performed.

3.1 *Thermal analyses*

The nucleating ability of the straw fibers on the crystallization process of iPP was tested by a non-isothermal crystallization experiment. All samples were heated from 30 °C to 200 °C at a scan rate of 20 °C/min and kept at this temperature for 10 min in order to destroy any trace of crystallinity (run I); afterwards the samples were cooled to 30 °C by using a prefixed scan rate (run II). Finally, a third run (run III), similar to run I, was performed. In Tab. 2 the thermal data obtained are shown and the following conclusions emerge:

i) In the first fusion cycle the crystallinity content of iPP is quite the same for the composites both in iPP and in iPPMA; furthermore the melting point of iPP is the same for the composites both in iPP and iPPMA. Differences in the values of melting point and X_c between iPP and iPPMA can be ascribed to the lower crystallinity content of iPPMA with respect to iPP, owing, probably, to the presence of maleic anhydride.

Tab. 2. Apparent melting point, crystallinity index and crystallization temperature of all samples[a].

Parameter	iPPMA neat (iPP neat)	iPPMA/straw 90/10	iPPMA/straw 80/20 (iPP/straw 80/20)	iPPMA/straw 70/30	iPPMA/straw 50/50 (iPP/straw 50/50)
T_m(°C)	158	159	159	160	159
	(166)		(167)		(165)
X_c(%)	35	35	36	35	37
	(42)		(39)		(42)
T_c(°C)	117	117	117	118	117
	(117)		(120)		(115)
X_c(%)	34	37	35	33	39
	(41)		(40)		(44)
T_m(°C)	153	156	155	153	153
	(162)		(161)		(162)
X_c(%)	31	34	33	32	32
	(39)		(39)		(42)

[a] Scan rate = 20 °C/min.

in the composites and by using all cooling scan rates.

iii) The run III, after non-isothermal crystallization, showed no variation of the X_c values with increasing fiber content, as found in run I.

3.2 *FTIR analyses*

Fig. 2 shows the spectrum of iPPMA as received and after activation by heating the film at 180 °C for 5–30 min. The non-activated sample shows a band at 1713 cm^{-1} with a shoulder at 1737 cm^{-1} ascribed to the dimeric form of dicarboxylic acids[16]. The thermal activation induces the appearance of two bands at 1785 and 1861 cm^{-1}, respectively, whose intensity increases as function of the activation time. These bands were attributed to a cyclic anhydride group[16].

In addition, the intensity of the band at 1713 cm^{-1} decreases, suggesting the transformation from the less reactive hydrolized acid form to the more reactive cyclic anhydride one.

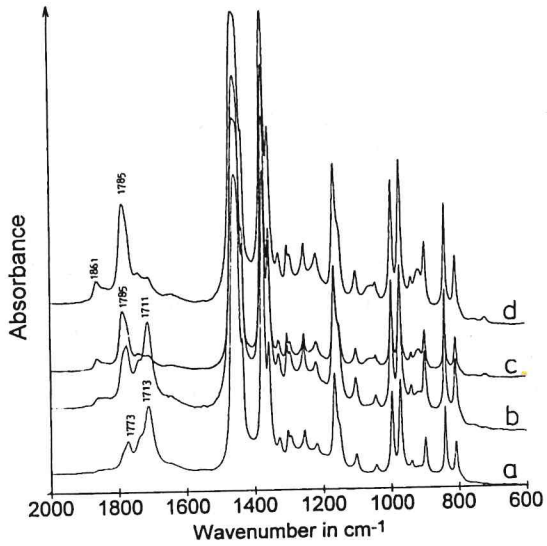

Fig. 2. FTIR spectra of iPPMA; as received (a), and after activation heating at 180 °C for 5 (b), 10 (c) and 30 min (d).

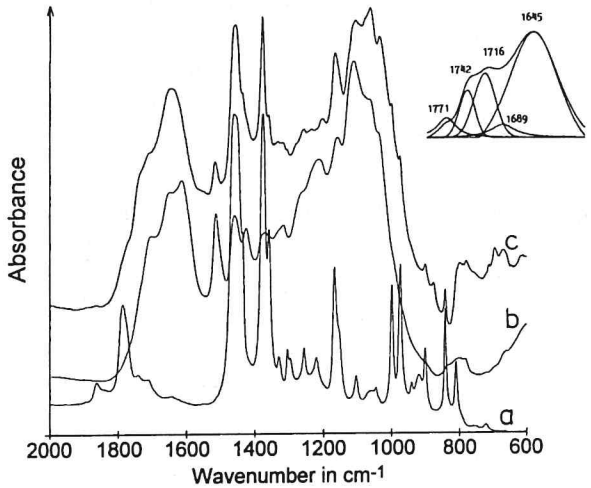

Fig. 3. FTIR spectra of (a) iPPMA activated at 180 °C for 30 min; (b) steam-exploded wheat straw; (c) iPPMA50/50. Insert shows a deconvoluted spectrum of (c).

Fig. 3 shows the spectra of the iPPMA copolymer (a), of the steam-exploded wheat straw (b) and of the straw/IPP composite (c).

The disappearance of the cyclic anhydride band is observed as well as the occurrence of some bands in the deconvoluted spectrum (see insert in Fig. 3) ranging from 1771 to 1645 cm^{-1}; the bands being not super-imposed with those of the wheat straw and attributed[17] to the presence of acid or ester groups. The latter are due to the reaction between the iPPMA copolymer and the hydroxy groups of the wheat straw confirming interface interaction between STEX straw and the iPPMA matrix.

3.3 Impact tests and fractographic analysis

The values of the critical strain energy release rate, G_c, and the critical stress intensity factor, K_c, for all examined samples, calculated according to the Linear Elastic Fracture Mechanics (LEFM)[13,14] theory, as a function of straw fiber content are shown in Tab. 3 and in Fig. 4, respectively. The values of K_c and G_c seem to linearly increase with increasing fiber content for iPPMA-based composites, while the K_c and G_c values of iPP-based composites remain almost constant.

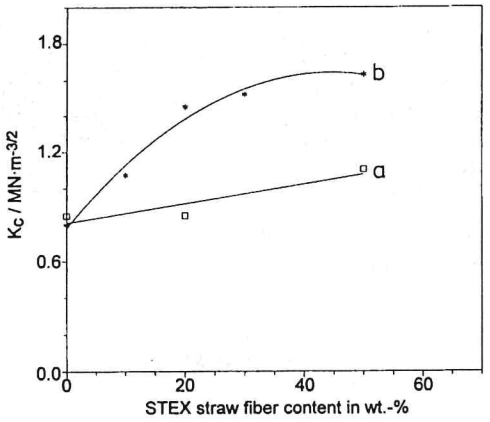

Fig. 4. Critical stress intensity factor, K_c, of (a) iPP and (b) iPPMA-based composites as function of fiber content (ASTM D256).

Tab. 3. Critical stress intensity factor (K_c) and critical strain energy release (G_c) of iPPMA and iPP-based composites (ASTM D256).

Parameter	iPPMA neat (iPP neat)	iPPMA/straw 90/10	iPPMA/straw 80/20 (iPP/straw 80/20)	iPPMA/straw 70/30	iPPMA/straw 50/50 (iPP/straw 50/50)
K_c ($MN/m^{-3/2}$)	0.80	1.07	1.45	1.52	1.63
	(0.85)		(0.80)		(1.10)
G_c ($kJ\ m^{-2}$)	0.23	0.53	0.74	0.77	0.86
	(0.40)		(0.40)		(0.50)

The strong performance of fracture parameters found in the iPPMA composites is probably due to a stronger chemical interfacial adhesion, owing to the presence of reactive radicals of maleic anhydride, but also its nucleating action producing a smaller size of spherulites and consequently a more pronounced presence of amorphous phases allows to absorb more energy during the fracture test[11].

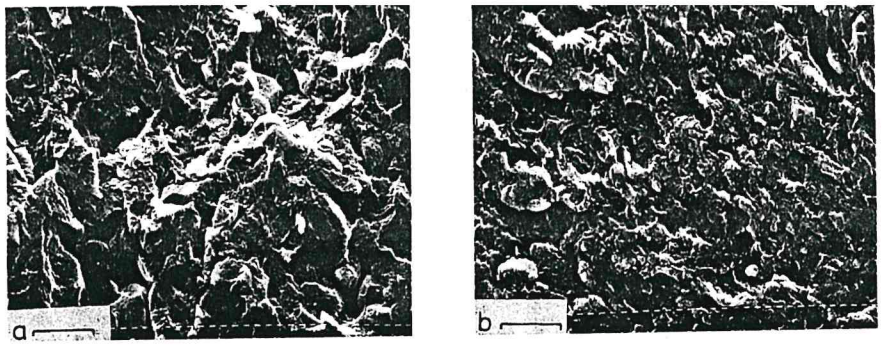

Fig. 5. Scanning electron micrographs of fracture surfaces of iPP and iPPMA samples; a) iPP, b) iPPMA; length of the bars: 100 μm.

The results on the fracture behavior can be interpreted on the basis of the fractographic analyses performed by SEM on the surface of notched specimens, the SEM micrographs were taken near the notch tip in the region of crack initiation. Fig. 5a and 5b show the fracture surfaces of the neat iPP and iPPMA, respectively. The fracture surface shows features of brittle materials. No evidence of shear bands is observed. The finer texture of the matrix seems to reveal a nucleating effect in iPPMA owing, probably, to the free maleic anhydride.

Fig. 6a and 6b show SEM micrographs of the iPP80/20 and iPPMA80/20 composites, respectively, and from the observation a better fiber-matrix adhesion in the case of iPPMA composite is evidenced with respect to iPP-based composites.

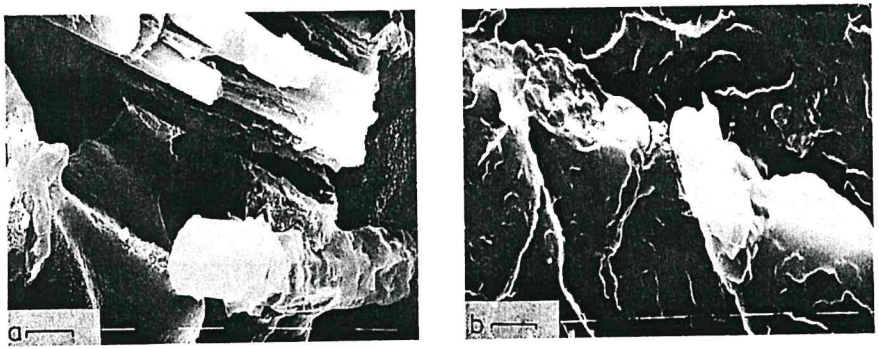

Fig. 6. Scanning electron micrographs of fracture surfaces of iPP and iPPMA-based composites; a) iPP80/20, b) iPPMA80/20; length of the bars: 10 μm.

Tensile properties such as tensile modulus (E), strength at break (σ_b) and elongation at break (ε_b) were evaluated from the stress-strain curves. The results are reported in Tab. 4. The trend of Young's modulus (E) versus the STEX straw fiber content for both the matrices is shown in Fig. 7. It can be observed that the stiffness of the material slightly increases with the fiber content for the iPPMA-based composites, while it remains almost constant in the case of iPP-based composites.

Tab. 4. Tensile properties of iPPMA and iPP-based composites (ASTM D638).

Parameter	iPPMA neat (iPP neat)	iPPMA/straw 90/10	iPPMA/straw 80/20 (iPP/straw 80/20)	iPPMA/straw 70/30	iPPMA/straw 50/50 (iPP/straw 50/50)
E (GPa)	1.2	1.3	1.4	1.5	1.6
	(1.2)		(1.2)		(1.1)
σ (MPa)	19.7	29.0	27.8	26.2	30.4
	(15.0)		(11.4)		(8.9)
ε (%)	1.9	2.9	2.7	2.2	2.4
	(1.4)		(1.0)		(0.9)

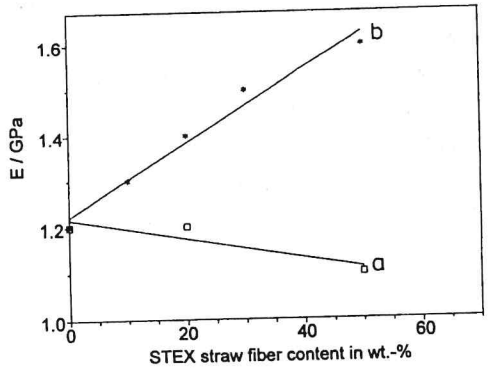

Fig. 7. Variation of Young's modulus versus fiber content; (a) iPP-based composites; b) iPPMA-based composites.

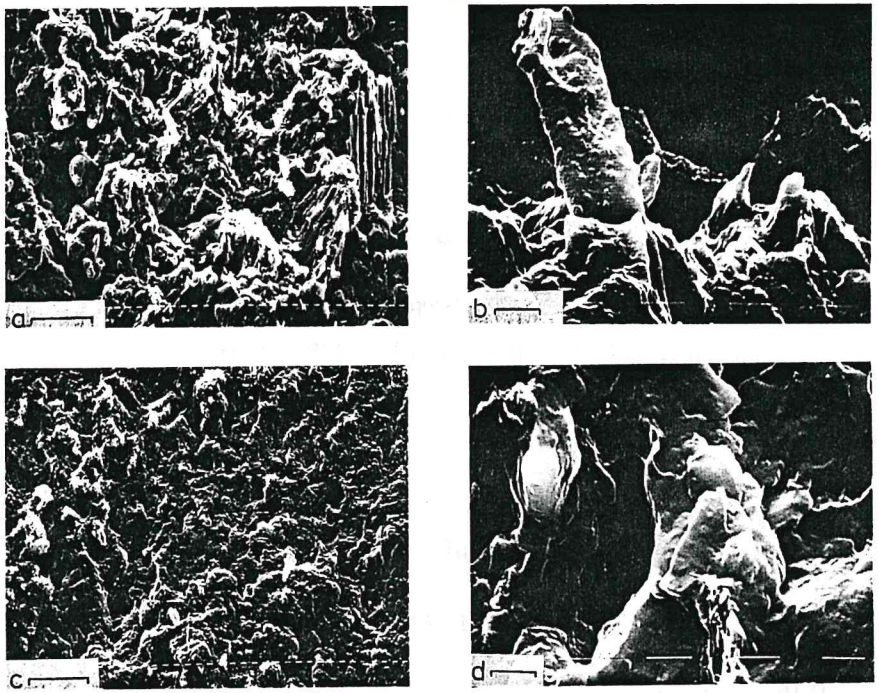

Fig. 8. Scanning electron micrographs of fractured surfaces of iPP and iPPMA-based composites; a) iPP80/20, b) iPP80/20, c) iPPMA80/20, d) iPPMA80/20; length of the bars: a, c) 160 μm; b, d) 10 μm.

As concerning the variation of strength at break (σ_b) as function of the straw fiber content, it is observed that the parameter decreases for iPP composites, whereas an opposite trend, in the case of iPPMA composites, is observed. This decrease found for iPP composites is likely due to weak interfacial bonding with the matrix. On the contrary, the high σ_b values for iPPMA-based composites have to be again attributed to the presence of maleic anhydride on the iPP backbone, that is able to graft the STEX fiber terminals.

The low values of elongation at break (ε_b) confirm a brittle behavior of all examined composites. Particularly, the iPP-based composites have shown a decrease of ε_b with increasing fiber content, whereas the iPPMA-based composites have shown only a slight increase.

In Fig. 8 the SEM micrographs of fractured samples (by tensile tests) for iPP80/20 (8a, 8b) and iPPMA80/20 (8c, 8d), respectively, are shown.

Both the samples evidenced a brittle behavior, but iPPMA-based samples seem to show a better dispersion of fibers together with a better covering with respect to iPP-based samples. Moreover, more regions of plastic deformations seem to appear in the case of iPPMA composites (see Fig. 8c).

3.5 Dynamic-mechanical tests

Fig. 9a shows the curves of storage modulus (E′) and loss modulus (tan δ) of the neat iPP matrix, iPP80/20 and iPP50/50 composites, respectively, as

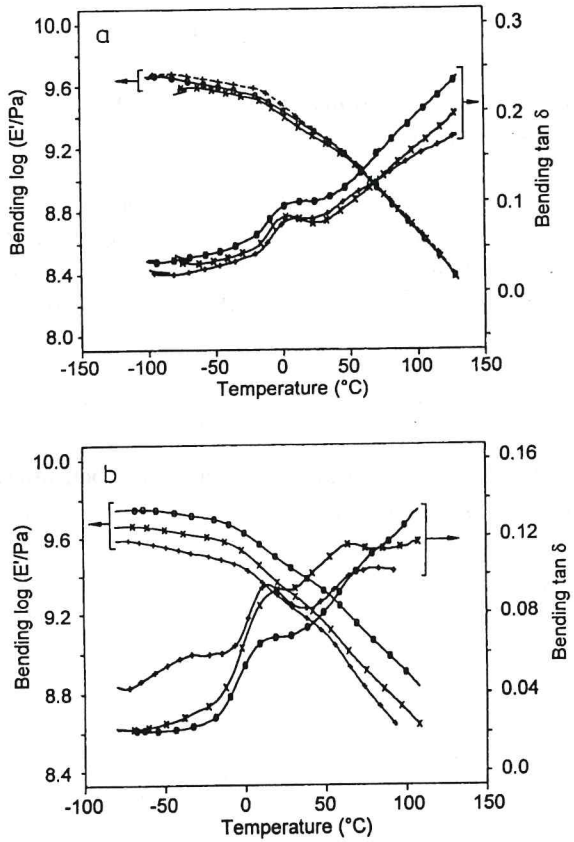

Fig. 9. DMTA storage modulus, E, and loss modulus, tan δ, vs. temperature; a) (+) neat iPP, (×) iPP80/20, (●) iPP50/50; b) (+) neat iPPMA, (×) iPPMA80/20, (●) iPPMA50/50.

function of temperature; in Fig. 9b the same curves of iPPMA-based composites are plotted. From the analysis of the figures it can be deduced that:

i) the modulus E′ is increased with increasing fiber content for iPPMA-based composites; in the opposite way the moduli are decreased in iPP-based composites. This is found to agree with tensile results.
   In all cases the storage modulus, E′, drops as the sample goes through the matrix-glass transition. The decrease of E′ with temperature is characteristic of semicrystalline polymers and the identical slopes of the curves indicate a similar degree of crystallinity owing to the same thermal treatment.
ii) over the temperature range in which the samples have been analysed, only the glass transition (T_g) is observed. The T_g, taken as the maximum of the tan δ peak, is not affected by the presence of filler both in iPP and iPPMA-based composites.

The loss modulus tan δ is related to the dissipated energy[18] by Eq. (1):

$$\tan\delta = \frac{E_d}{(E_0^2 - E_0^2)^{1/2}} \tag{1}$$

where E_0 is the total work done during a cycle of oscillation, and E_d is its irreversibly lost component, i.e. the fraction of the deformation energy dissipated as heat.

An attempt to quantify the adhesion between fiber and matrix can be derived from the assumption[18] that a good adhesion reduces the mobility of the polymer chains in the interface, with respect to the matrix, and consequently the ability to dissipate energy. As first approximation it is assumed (Eq. (2)):

$$\tan\delta_c = v_f \tan\delta_f + v_i \tan\delta_i + v_m \tan\delta_m \tag{2}$$

where the subscripts c, f, i, m denote composite, fiber, interface and matrix, respectively, and v is the volume fraction. Owing to lower elongation at break of the fiber, we also assume (Eq. (3)):

$$\tan\delta_f = 0 \tag{3}$$

So, it can be written:

$$A = \frac{v_i}{1 - v_f}\tan\delta_i = \frac{1}{1 - v_f}\frac{\tan\delta_c}{\tan\delta_m} - 1 \tag{4}$$

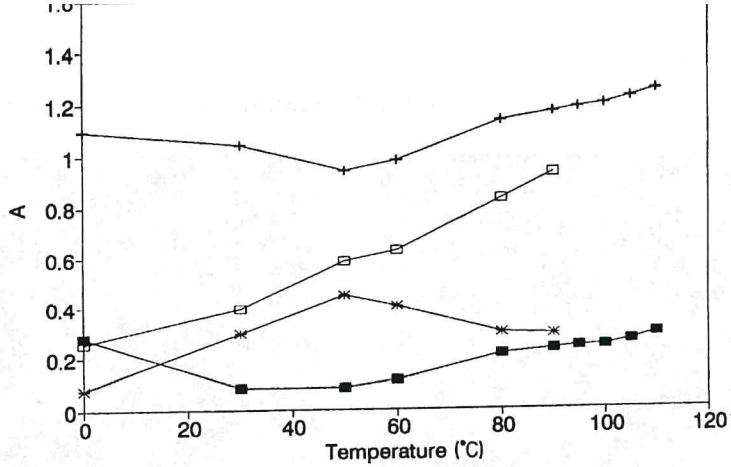

Fig. 10. Parameter of interaction, A; (■) iPP80/20, (*) iPPMA80/20, (+) iPP50/50, (□) iPPMA50/50.

Strong interactions between fiber and matrix at the interface reduce the mobility of the polymer chains, with respect to that in the bulk matrix; thus reduce $\tan\delta_i$ and consequently A. The values of A vs. temperature for the composites iPP80/20, iPP50/50, iPPMA80/20 and iPPMA50/50 are shown in Fig. 10.

If the straw content is low (iPP80/20, iPPMA80/20), no difference in the trend can be pointed out. In the opposite way, for high straw content, the A values increase with increasing temperature for the iPPMA-based composite, indicating a deterioration of the degree of adhesion, but the values always are lower than for the iPP50/50 sample, indicating a better adhesion for iPPMA-based composites. The reducing in adhesion occurs when the thermal contraction of the matrix around the fibers has been released.

3.6 Water absorption

The water absorption is one of the most serious problems that prevents a wide use of natural fiber composites; in fact, in wet conditions, this phenomenon strongly decreases the mechanical performances of composites. This latter can be attributed to the fact that, generally, the lignocellulosic materials

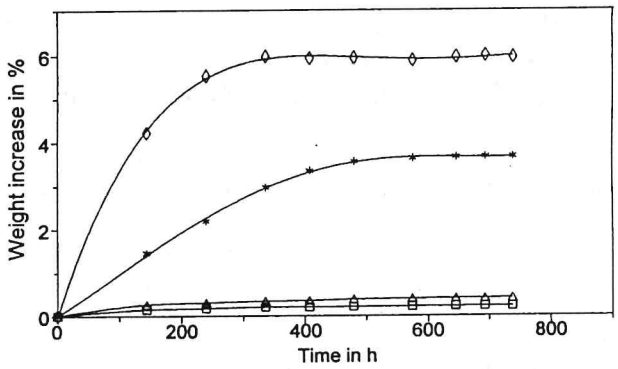

Fig. 11. Water absorption test: increase of weight of the samples vs. time; (□) neat iPP, (△) neat iPPMA, (◇) iPP50/50, (*) iPPMA50/50.

are hydrophilic and the plastics are hydrophobic. Consequently, the resulting interface bond between natural fibers and polymer is too weak. Only by creating a stronger interface between matrix and reinforcement material, it is possible to reduce the hygroscopicity of lignocellulosic-based materials.

Water absorption tests on our samples were performed in the following way. Specimens having thickness of 1 mm (W = 70 mm × L = 110 mm) of iPP, iPPMA, iPP50/50 and iPPMA50/50 samples have been kept immersed at room temperature for one month and the increase of weight due to the water absorbed was periodically measured. The results of the tests are reported in Fig. 11. The findings show that the two homopolymers (iPP and iPPMA) absorb about the same amount of water. On the contrary a lower quantity of water can penetrate into the iPPMA50/50 composite with respect to the iPP-based composite (iPP50/50), owing to a better adhesion of the fibers to the matrix. Tensile tests, after this treatment, were also performed. The results are shown in Tab. 5 and the following can be pointed out:

i) A constant decrease of tensile properties (E, σ_b and ε_b) for all wet samples was observed (compare Tab. 4 and 5).

ii) Only a slight worsening of tensile strength at break was found in the case of iPPMA50/50. The parameter (σ_b) can give an indication of the resulting fiber-matrix adhesion in the composites, confirming, in our case, the positive action of maleic anhydride groups that allow to improve the interface between the two phases, avoiding an easy penetration of water molecules into the composites.

Tab. 5. Tensile properties of iPPMA and iPP-based composites (ASTM D638) after water absorption test.

Parameter	iPPMA neat (iPP neat)	iPPMA/straw 50/50 (iPP/straw 50/50)
E (GPa)	1.1	1.3
	(1.1)	(1.0)
σ (MPa)	12.7	28.4
	(11.3)	(6.1)
ε (%)	1.3	1.7
	(1.4)	(0.7)

Conclusions

iPP and iPPMA-based composites reinforced with STEX wheat straw fibers were prepared by means of compression molding and the thermal and mechanical behavior as well as the interfacial adhesion between polymer lignocellulosic material were examined.

The following conclusions from the results reported can be drawn: FTIR analysis shows the presence of ester linkages in the case of iPPMA composites, allowing a superior interfacial adhesion with respect to iPP-based composites.

The presence of STEX straw fibers in both matrices (iPP and iPPMA) does not produce a worsening of thermal properties of composites (T_m, X_c and T_c).

The fracture toughness parameters (K_c and G_c) increase with STEX straw fiber content, especially in the case of iPPMA composites.

The mechanical properties, as shown by tensile tests, for iPPMA composites increase with the straw fiber content; an opposite trend in the case of iPP composites series is observed. These results have been also confirmed by fractographic analyses performed by SEM.

The presence of maleic groups is able to create a strong interface between polypropylene and lignocellulosic material, limiting the penetration of water molecules under wet conditions.

The authors thank Ms. M. T. Palma for her help in performing the FTIR experiments. The work has been granted in the framework of an EC-ECLAIR project (AGRE CT 90-0044). The authors also thank "Progetto Finalizzato Chimica Fine II" of C.N.R.

F. Zadorecky, A. J. Michels, Polym. Compos. [illegible]
2 J. F. Kennedy, G. O. Phillips, P. A. Williams, Wood Processing and Utilization, Ellis Horwood, London 1989
3 D. Maldas, B. V. Kokta, Int. J. Polym. Mater. **14** (1990) 165
4 M. Dalväg, C. Klason, H. E. Strömvall, Int. J. Polym. Mater. **11** (1985) 9
5 C. Klason, J. Kubát, H. E. Strömvall, Int. J. Polym. Mater. **10** (1984) 159
6 B. Focher, A. Marzetti, V. Crescenzi, "Steam explosion techniques: fundamentals and applications", Gordon and Breach Sci. Publ., Philadelphia **1991**
7 R. P. Overend, E. Chornet, Philos. Trans. R. Soc. London A: **321** (1987) 523
8 R. M. Marchessault, S. Coulomba, H. Morikawa, D. Robert, Can. J. Chem. **60** (1982) 2372
9 D. Maldas, B. V. Kokta, Polym. Eng. Sci. **31** (1991) 1351
10 M. Tanahashi, J. Wood Res. **77** (1991) 49
11 S. N. Maiti, R. Subbarao, Int. J. Polym. Mater. **15** (1991) 1
12 R. P. Quirk, M. A. A. Alsamarraie, Polym. Handb., 3rd ed. (1989), p. V-31
13 A. J. Kinloch, R. J. Young, "Fracture Behaviour of Polymers", Applied Science, London 1983
14 F. Coppola, R. Greco, G. Ragosta, J. Mater. Sci. **21** (1986) 1775
15 J. K. Kauppinen, D. J. Moffat, H. H. Mantsch, D. Cameron, Anal. Chem. **53** (1981) 1454
16 J. M. Felix, P. Gatenholm, J. Appl. Polym. Sci. **42** (1991) 609
17 E. L. Saier, L. Petrakis, I. R. Cousins, W. J. Helman, J. F. Itzel, J. Appl. Polym. Sci. **12** (1968) 2191
18 J. Kubát, M. Rigdahl, M. Welander, J. Appl. Polym. Sci. **39** (1990) 1527